Desalination and Water Treatment
www.deswater.com
doi: 10.1080/19443994.2014.895778

54 (2015) 2241–2251
May

Taylor & Francis
Taylor & Francis Group

Equilibrium and thermodynamics studies for decolorization of Reactive Black 5 (RB5) by adsorption onto MWCNTs

Edris Bazrafshan[a], Ferdos Kord Mostafapour[a], Somaiieh Rahdar[a,*], Amir Hossein Mahvi[b,c,d]

[a]*Health Promotion Research Center, Zahedan University of Medical Sciences, Zahedan, Iran, Tel. +989158940786; email: Rahdar89@gmail.com*
[b]*School of Public Health, Tehran University of Medical Sciences, Tehran, Iran*
[c]*Center for Solid Waste Research, Institute for Environmental Research, Tehran University of Medical Sciences, Tehran, Iran*
[d]*National Institute of Health Research, Tehran University of Medical Sciences, Tehran, Iran*

Received 5 August 2013; Accepted 11 February 2014

ABSTRACT

At present study, multi-walled carbon nanotubes were used as an adsorbent for Reactive Black 5 (RB5) removal from aqueous solutions. The influence of important parameters including initial pH, concentration of dye, contact time, adsorbent dosage, and temperature has been investigated in order to find the optimum adsorption conditions. The results show that all the parameters have a strong effect on the adsorption of RB5 onto adsorbent. Adsorption kinetics was best described by the pseudo-second-order model. In addition, equilibrium data were better represented by Freundlich isotherm among Langmuir, Freundlich, Temkin, and Dubinin–Radushkevich equilibrium isotherm models. The negative values of free-energy change confirmed the feasibility of the process and the spontaneous nature of adsorption. Furthermore, from the magnitude of ΔH, the process was found to be endothermic physisorption.

Keywords: Decolorization; Reactive Black 5; Adsorption; MWCNTs

1. Introduction

Dyes are one of the most hazardous chemical compound classes found in industrial effluents and among them, azo dyes represent an important portion of the commercial synthetic dyes. Azo dyes are synthetic organic compounds widely used in textile dyeing, paper printing, and other industrial processes, such as the manufacture of pharmaceutical drugs, toys, and foods including candies. This chemical class of dyes, which is characterized by the presence of at least one azo bond (–N=N–) bearing aromatic rings, dominates the worldwide market of dyestuffs with a share of about 70% [1]. In addition, most azo dyes are mutagenic and carcinogenic to living organisms [2,3]. These dyes also cause serious ecological problems; for example, they significantly affect the photosynthetic activity of aquatic plants by reducing light penetration, and they may be toxic to some aquatic organisms [4].

In addition, azo dyes are highly recalcitrant to conventional wastewater treatment processes. In fact, as much as 90% of reactive azo dyes could remain unaffected after activated sludge treatment [5].

*Corresponding author.

1944-3994/1944-3986 © 2014 Balaban Desalination Publications. All rights reserved.

Unsuitable treatment and disposal of wastewaters from textile, dyeing, printing, ink, and related industries have provoked strict environmental concerns all over the world [6–8]. Currently, there are a number of methods available for treatment of dye-containing wastewater, such as membrane processes [6,9], photochemical and sonochemical processes [10], coagulation and flocculation [11], and biological processes [12]. However, some of these methods are limited due to their high operational costs and problems.

The adsorption technique has been found not only to be effective, but also practical in application for the dye-containing wastewater treatment, due to its high efficiency, simplicity, ease of operation, and the availability of a wide range of adsorbents [13,14]. Nevertheless, application of adsorption process is limited by the high price of some adsorbents and the large amounts of wastewater normally involved. Activated carbon is the most popular and widely used dye adsorbent but it suffers from several drawbacks, such as its high cost of both manufacturing and regeneration, and it is ineffective against disperse and vat dyes [15].

Carbon nanotubes (CNTs), ever since their discovery, have attracted extensive attention due to their unique physicochemical and electrical properties. CNTs, divided into two groups of single-walled carbon nanotubes and multi-walled carbon nanotubes (MWCNTs), are used as a new and small-sized adsorbent with a hollowed and stratified structure [16]. This new type shows a higher capacity for adsorption compared to the activated carbon, and it can remove dyes and other pollutants from wastewater [17,18].

The aim of this study was to evaluate adsorption of Reactive Black 5 (RB5) from aqueous solution using MWCNTs. Batch experiments were performed to evaluate the effects of various operating parameters including initial pH of solution, adsorbent dosage, RB5 concentration, contact time, and temperature on the adsorption capacity. Additionally, equilibrium isotherms and thermodynamic parameters were explored to describe the experimental data.

2. Materials and methods

2.1. Chemicals and reagents

RB5 is an anionic dye with molecular weight of 991.82 g/mol and maximum absorption (λ_{max}) 597 nm. The RB5 ($C_{26}H_{21}N_5Na_4O_{19}S_6$) used in this work was of analytical grade (Merck, Germany). The chemical formula of RB5 is shown in Fig. 1. This dye is characterized as a diazo compound, which bears two sulphonate and two sulphatoe-thylsulphon groups that have negative charges in an aqueous solution. For treatment experiments, the dye solutions with concentrations in the range of 10–200 mg/L were prepared by successive dilution of the stock solution (1,000 mg/L) with distilled water. All other chemicals used in this study were of analytical grade.

2.2. Adsorbent preparation

MWCNTs (provided from Research Institute of Petroleum Industry (RIPI), Tehran, Iran), were selected as adsorbents to study the adsorption characteristics of RB5 from aqueous solutions. On the basis of the information provided by the manufacturer, the MWCNTs were synthesized by catalytic chemical vapor deposition method. The size and morphology of MWCNTs were examined by scanning electron microscope (SEM) (JEOL JSM-6700F) and transmission electron microscopy (TEM) (using a Philips XL 30 ESEM). Figs. 2 and 3 show the SEM and TEM images of $MWCNT_S$. The size of the outer diameter for the MWCNTs was 10–30 nm. The length of MWCNTs was 10 μm. Furthermore, specific surface area of MWCNTs was more than 270 $m^2 g^{-1}$, and the mass ratio of the amorphous carbon of MWCNTs was less than 5%.

Because CNTs had the amorphous carbon, the adsorption rate is very low, therefore, carbon nanotubes should be purified. In order to functionalize MWCNTs, 1.0 g of the as-received MWCNTs was dispersed in 60 mL of nitric acid (65 wt.%) in a 100 mL round-bottom flask to get a homogeneous mixture and then refluxed for 48 h at 90°C. After that, the mixture was filtered and washed with distilled water until the pH of the filtrate was equal to seven. The resulting functionalized MWCNTs were dried under vacuum for 20 h at 45°C. Fig. 4 shows an overview of the obtained FT-IR for raw and acid-modified-MWCNTs sample.

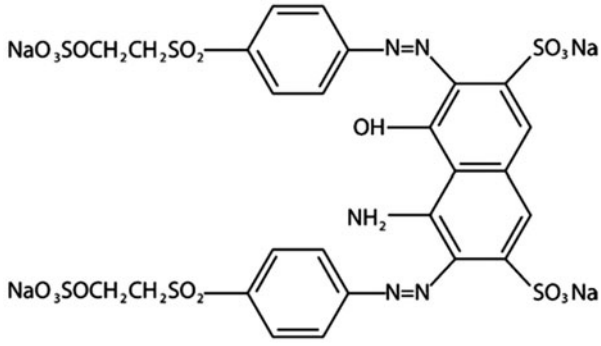

Fig. 1. Structure of RB5.

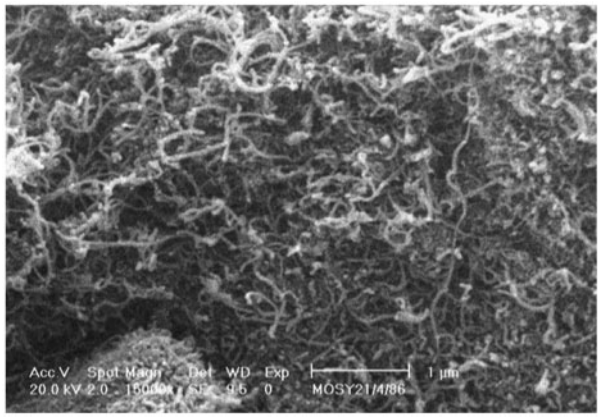

Fig. 2. SEM image of MWCNTs sample.

2.3. Dye removal experiments

Experiments for RB5 dye removal with the MWCNTs were carried out as batch tests in 250 mL flasks under magnetic stirring. Each test consisted of preparing a 100 mL of dye solution with a desired initial concentration (10–200 mg/L) and pH (2–12) by diluting the stock dye solution with distilled water, and transferring it into the beaker on the magnetic stirrer. The pH was adjusted with HCl or NaOH. The final pH of the solution after adsorption equilibrium was nearly the same as before. A known mass of MWCNTs (adsorbent dosage) was then added to the solution, and the obtained suspension was immediately stirred for a predefined time. After the desired contact time, the samples were withdrawn from the mixture using a micropipette and centrifuged for 5 min at 6,000 rpm. The final concentrations of the dye which remained in the solution were determined by spectrophotometric method (using UV–Vis spectrophotometer (T80 PG Instruments Ltd)).

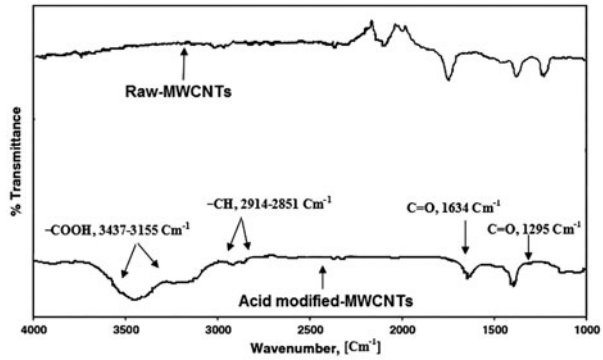

Fig. 4. FT-IR spectra of MWCNTs sample.

Absorbance measurements were made at the maximum wavelength of RB5 dye at 597 nm. The reproducibility during concentration measurements was ensured by repeating the experiments thrice under identical conditions and the average values were calculated. Standard deviations of experiments were found to be within ±3.0%. The amount of adsorbed dye, q_e (mg g^{-1}), under different conditions was calculated as follows:

$$q_e = \frac{(C_0 - C_e)V}{M} \tag{1}$$

where C_0 and C_e are the initial and equilibrium liquid-phase concentration of RB5 (mg/g), respectively. V is the volume of the solution (L) and M is the amount of adsorbent used (g).

To express the percent of dye removal, the following equation was used:

$$\% = \frac{(C_0 - C_f)}{C_0} \times 100 \tag{2}$$

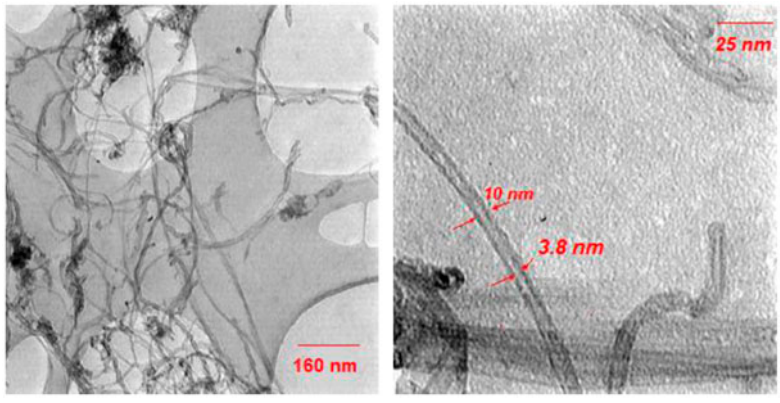

Fig. 3. TEM image of MWCNTs sample.

where C_0 and C_f represent the initial and final (after adsorption) dye concentrations, respectively. All tests were performed in duplicate to insure the reproducibility of the results; the mean of the two measurements is reported. The plot of equilibrium adsorption capacity against equilibrium concentration in the liquid phase graphically depicts the equilibrium isotherm.

3. Results and discussion

3.1. Effect of initial pH on the RB5 adsorption

RB5 is an anionic dye, which exists in the aqueous solution in the form of negatively charged ions. As a charged species, the degree of its adsorption onto the adsorbent surface is primarily influenced by the surface charge on the adsorbent, which in turn is influenced by the solution pH. Consequently, the solution pH is an important parameter during the dye-adsorption process. For example, Ghaedi et al. reported that adsorption of bromothymol blue dye on MWCNTs adsorbent depends highly on pH [19].

To study the influence of solution pH on the adsorption capacities of MWCNTs for RB5, experiments were carried out using various initial pHs varying from 2 to 12, at constant initial dye concentration of 50 mg/g, adsorbent dose of 0.1 g/L, and contact time of 60 min. From Fig. 5, it is observed that the adsorption was highly dependent on the pH of the solution, and indicated that the RB5 dye-removal efficiencies decreased with the increase of solution pH.

As can be seen from Fig. 5, the maximum adsorption capacity of the adsorbent was 373.9 mg/g at pH 2 and initial concentration of 50 mg/g, when 74.8% of the dye was removed. In contrast, removal efficiency at pH 12.0 was only 42.1% and adsorption capacity was 210.6 mg/g. Similar result was reported by Dehghani et al. [20]. The dissolved RB5 dye is negatively charged in aqueous solution, because it possesses two sulphonate groups ($-SO_3^-$). Thereby, the adsorption of this dye takes place when the adsorbents present a positive surface charge. On the other hand at lower pHs, more protons would be available, thereby a significantly high electrostatic attraction existed between the positively charged adsorption sites and negatively charged dye anions, which caused the enhanced dye adsorption [21,22]. But as the pH of solution increased, besides the decrease of negative charge of reactive dyes, the positive charge of adsorbent surface also decreased due to the abundance of OH^-, which can weaken the reaction of dye and adsorbent, and thereby causing a decrease in adsorption. In order to continue the adsorption studies, the initial pH was fixed at 2.0.

3.2. Effect of adsorbent dose on the RB5 adsorption

The adsorbent dosage is an important parameter because this determines the capacity of the adsorbent (MWCNTs) for a given initial RB5 concentration. Therefore to evaluate the effect of adsorbent dose on the adsorption of BB5, 0.1–1.0 g/L MWCNTs were used for adsorption experiments at fixed initial pH (pH 2), initial dye concentration (50 mg/g), and temperature 20°C for 60 min. As it can be seen from Fig. 6, the uptake of the dye increased rapidly with increased amount of adsorbent from 0.1 to 0.4 g and slowed down from 0.4 to 1.0 g. This result can be explained by the fact that the sorption sites remain unsaturated during the sorption; whereas the number of sites available for sorption site increases by increasing the adsorbent dose. A maximum of 97.88% (48.94 mg/g) removal of the dye was observed at adsorbent concentration of 1.0 g/L.

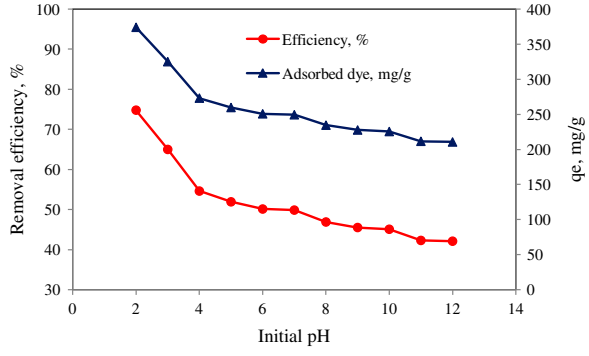

Fig. 5. Effect of initial pH on RB5 adsorption onto MWCNTs.

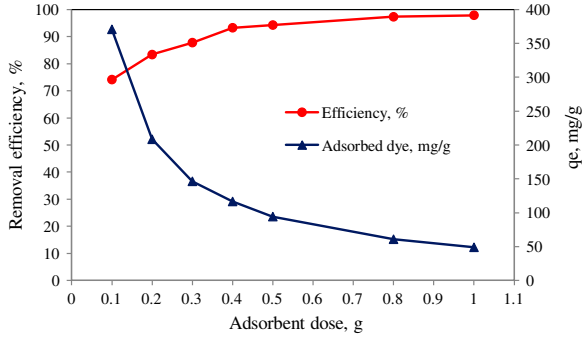

Fig. 6. Effect of adsorbent dosage on RB5 adsorption onto MWCNTs.

Obviously, the RB5 adsorbed per gram of adsorbent decreased rapidly with an increase in the amount of adsorbent (maximum adsorption capacity equal 370.7 mg/g was observed at minimal adsorbent dose 0.1 g/L). It can be related to the fact that fixed dye concentration (50 mg/L) led to unsaturated active site on adsorbent surface and increase in the adsorbent concentrations caused particle aggregation [23]. Similar findings were reported by other researchers [24–26].

3.3. Effect of contact time and initial dye concentration

The adsorbate concentration and contact time between adsorbent and adsorbate species play a significant role in the process of removal of pollutants from aqueous solutions by adsorption at a particular temperature and pH. The effects of initial dye concentration and contact time on the removal rate of RB5 by the MWCNTs are shown in Figs. 7 and 8.

The effect of contact time on the RB5 adsorption by the MWCNTs was investigated for 210 min at different initial dye concentrations. It is clear from Fig. 7 that the removal of RB5 has increased with the increase in contact time at all initial RB5 dye concentrations. For the first 20 min, the adsorption uptake was rapid (59–86%), then it proceeds at a slower adsorption rate and finally it attains equilibrium at 120 min. Also, it can be seen from the Fig. 7, that the equilibrium period remains unaltered with the change of initial concentration of the dye solution. This is obvious from the fact that a large number of surface sites are available for adsorption at the initial stages and after a lapse of time, the remaining surface sites are difficult to be occupied because of repulsion between the solute molecules of the solid and bulk phases. Furthermore, the obtained removal curves were single, smooth, and continuous, indicating monolayer coverage of dye on the surface of adsorbent [27].

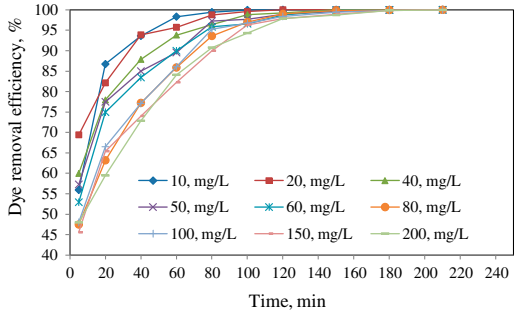

Fig. 7. Effect of contact time for the adsorption of RB5 onto MWCNTs (trend of dye removal).

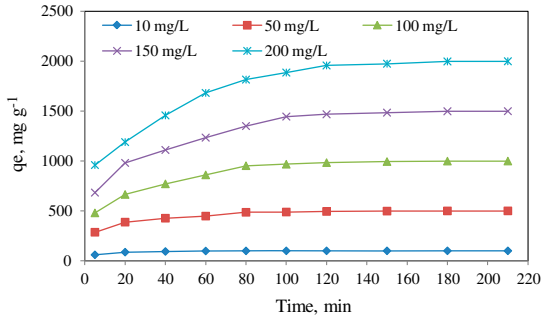

Fig. 8. Effect of contact time for the adsorption of RB5 onto MWCNTs (trend of adsorbed dye).

As shown in Figs. 7 and 8, when the initial dye concentration is increased, the percent of dye removal decreased. In contrast when the initial dye concentration is increased, the amounts of adsorbed dye also increased (Fig. 8), so the removal of dye depends on the concentration of the dye. For example, when the initial RB5 concentration increases from 10 to 200 mg/L (at contact time 5 min), the equilibrium sorption capacity of MWCNTs increased from 59.91 to 959.2 mg/g. This increase in the proportion of removed dye may be probably due to equilibrium shift during sorption process. In fact, the initial dye concentrations provide an important driving force to overcome the mass-transfer resistance of the dye between the aqueous phases and the solid phases, so increasing initial concentrations would enhance the adsorption capacity of dye. Furthermore, the time taken to reach equilibrium was equal for all the initial dye concentrations used, which was 120 min. This finding is supported by the study carried out by Osma et al. [28], who reported that the initial concentration of dyes had only a small influence on the time of contact necessary to reach equilibrium in the adsorption study of RB5 by sunflower seed shells.

3.4. Effect of temperature on RB5 dye adsorption and thermodynamic studies

The effect of temperature on RB5 dye adsorption was investigated at (293–323 °K). As it can be seen from Fig. 9, the removal efficiency of RB5 for all initial dye concentrations were increased, when the temperature was increased from 293 to 323 °K. Increasing the temperature is known to increase the rate of diffusion of the adsorbate molecules across the external boundary layer and in the internal pores of the adsorbent particle, owing to the decrease in the viscosity of the solution. In addition, change of temperature will change the equilibrium capacity of the adsorbent for a

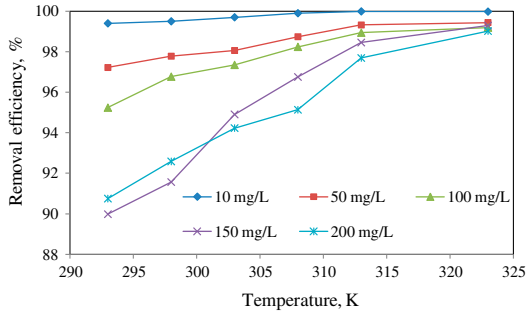

Fig. 9. Effect of temperature on RB5 dye adsorption onto MWCNTs.

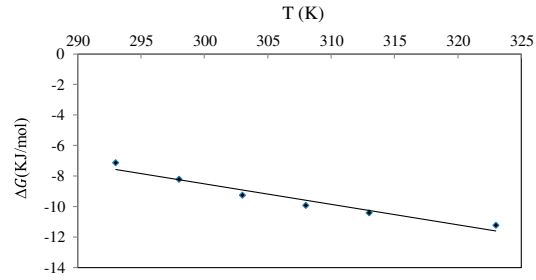

Fig. 10. Plot of Gibbs free energy change, ΔG°, vs. temperature, T.

particular adsorbate [29]. Similar findings were reported by Khodaie et al. [30].

Thermodynamic considerations of an adsorption process are necessary to conclude whether the process is spontaneous or not. Gibb's free energy change, ΔG°, is the fundamental criterion of spontaneity. Reactions are spontaneous at a given temperature if ΔG° is a negative value. The thermodynamic parameters of Gibb's free energy change, ΔG°, enthalpy change, ΔH°, and entropy change, ΔS°, for the adsorption processes are calculated using the following equations:

$$\Delta G^{\circ} = -\mathrm{RT} \ln K_a \tag{3}$$

$$\Delta G^{\circ} = \Delta H^{\circ} - T\Delta S^{\circ} \tag{4}$$

where R is universal gas constant (8.314 J mol/K) and T is the absolute temperature in K.

The thermodynamic parameter, Gibb's free energy change, ΔG°, is calculated using K_a obtained from Freundlich Eq. (8) and is shown in Table 1.

A plot of Gibb's free energy change, ΔG°, against temperature, T, was found to be linear (Fig. 10). The enthalpy change, ΔH°, and the entropy change, ΔS°, for the adsorption process were obtained from the intercept and slope of Eq. (4) and found to be 31.2 kJ/mol and 0.156 kJ/mol/K, respectively. The negative values of ΔG° confirm the feasibility of the process and also the spontaneous nature of adsorption with a high preference of RB5 by MWCNTs. Furthermore, the decrease in the negative value of ΔG° with an increase in temperature indicates that the adsorption process of RB5 on MWCNTs becomes more favorable at higher temperatures [31].

Table 1
Thermodynamics parameters for RB5 adsorption on MWCNTs

Temperature (°K)	ΔG° (kJ/mol)	ΔH° (kJ/mol)	ΔS° (kJ/mol/K)
293	−14.63		
298	−15.2		
303	−15.9	31.2	0.156
308	−16.8		
313	−17.96		
323	−19.08		

Adsorption process can be classified as physical adsorption and chemisorption by the magnitude of the enthalpy change. It is accepted that if magnitude of enthalpy change is lesser than 84 kJ/mol, then the adsorption is physical. However chemisorption takes place in the range of 84–420 kJ/mol [32]. From these results (Table 1) it is clear that physisorption is much more favorable for the adsorption of RB5.

Also, the positive value of ΔH° indicates that the adsorption reaction is endothermic. Entropy has been defined as the degree of chaos of a system. The positive value of ΔS° suggests that some structural changes occur on the adsorbent and the randomness at the solid–liquid interface in the adsorption system increases during the adsorption process [33].

3.5. Kinetics of the adsorption process

The reaction rate is described by adsorption kinetics. Adsorption kinetics is important in characterizing the efficiency of a sorbent for use in the adsorption process. The kinetics of the removal of RB5 with MWCNTs was investigated to understand the behavior of the sorbent. Fig. 11 illustrates the adsorption kinetics of RB5. The removal rate of RB5 was fast during the initial stages of the adsorption processes, especially for an initial dye concentration of 150 and 200 mg/L. However, the adsorption equilibrium was reached at 120 min for all the five concentrations tested. The kinetic data in Fig. 11 were treated with a pseudo-second-order rate equation. The second-order kinetic model [34,35] is expressed as:

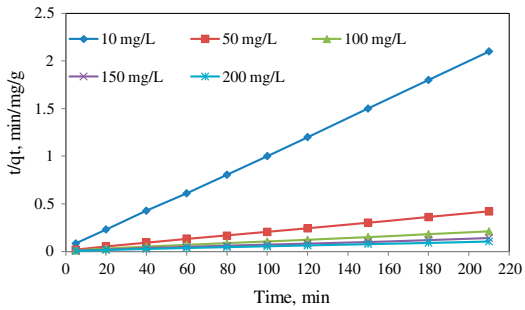

Fig. 11. Pseudo-second-order kinetic plots for RB5 adsorption on MWCNTs at different initial concentration of dye (dose = 0.01 g, pH 2, time = 5–210 min, and concentration = 10–200 mg/L in 100 mL of synthetic sample).

$$\frac{t}{q_t} = \frac{1}{K_2 q_e^2} + \frac{t}{q_e} \tag{5}$$

where k_2 is the pseudo-second-order rate constant (g/mg/min); q_e the quantity of dye adsorbed at equilibrium (mg/g); q_t the quantity of dye adsorbed at time t (mg/g), and t is the time (min).

As it can be seen from Fig. 11, the data fitted well with the second-order kinetics model ($R^2 > 0.99$). Also, the calculated qe values agree very well with the experimental data (Table 2). Similar kinetic results were reported in the biosorption of RB5 by powdered active carbon and fly ash [34] and RB5 biosorption by sunflower seed shells [28]. Investigations have shown that most adsorption systems at different concentrations of pollutants are consistent with this system.

3.6. Equilibrium adsorption isotherm

An important physiochemical aspect in terms of the evaluation of sorption processes is the sorption equilibrium. In fact, the isotherm provides a relationship between the concentration of dye in solution and the amount of dye adsorbed on the solid phase when both phases are in equilibrium. In order to investigate the adsorption isotherm, four equilibrium isotherms were analyzed: the Langmuir, Freundlich, Temkin, and Dubinin–Radushkevich isotherm.

Table 2
Kinetic parameters for the adsorption of RB5 by MWCNTs for different initial RB5 concentrations at pH 2

RB5 concentration (mg/L)	K_2	q_e (mg/g)	R^2
10	0.0276	0.0098	0.9999
50	0.0123	0.0019	0.9995
100	0.0098	0.0009	0.9985
150	0.008	0.0006	0.9976
200	0.0063	0.0005	0.9975

3.6.1. Langmuir isotherm

The Langmuir isotherm model assumes monolayer adsorption onto an adsorbent surface containing a finite number of identical sorption sites and without interaction between adsorbed molecules which is presented by the following equation:

$$q_e = \frac{q_m K_l C_e}{1 + K_l C_e} \tag{6}$$

where q_e is the amount of metal adsorbed per specific amount of adsorbent (mg/g), C_e is equilibrium concentration of the solution (mg/L), and q_m is the maximum amount of RB5 dye required to form a monolayer (mg/g). The Langmuir equation can be rearranged to linear form for the convenience of plotting and determining the Langmuir constants (K_l) and maximum monolayer adsorption capacity of MWCNTs (q_m). The values of q_m and K_l can be determined from the linear plot of $1/q_e$ vs. $1/C_e$:

$$\frac{1}{q_e} = \frac{1}{q_m} + \frac{1}{q_m K_l}\frac{1}{C_e} \tag{7}$$

3.6.2. Freundlich isotherm

The Freundlich equation is purely empirical, based on sorption on heterogeneous surface, which is commonly described by the following equation:

$$q_e = K_f C_e^{1/n} \tag{8}$$

where K_f and $1/n$ are the Freundlich constants related to adsorption capacity and adsorption intensity, respectively. The Freundlich equilibrium constants evaluated from the intercept and the slope, respectively, of the linear plot of log q_e vs. log C_e were based on experimental data. The Freundlich equation can be linearized in logarithmic form for the determination of the Freundlich constants as shown below:

$$\log q_e = \log K_f + \frac{1}{n}\log C_e \tag{9}$$

Table 3
Isotherm parameters for adsorption of RB5 onto MWCNTs at various temperatures

	293 °K	298 °K	303 °K	308 °K	313 °K	323 °K
Langmuir isotherm						
q_m (mg/g)	1,054.05	1,082.07	1,043.22	994.18	959.17	980.84
k_l (L/ mg)	1.73	2.02	3.51	11.16	116.35	56.72
R^2	0.9885	0.9889	0.9858	0.9828	0.9799	0.9806
Freundlich isotherm						
k_f	406.51	460.83	548.63	707.17	994.03	1217.79
n	2.03	2.01	2.03	2.31	2.89	2.39
R^2	0.9945	0.9892	0.996	0.9937	0.9743	0.9599
Temkin isotherm						
K_T	3.0578E–281	0.0	0.0	0.0	0.0	0.0
B	0.0032	0.0031	0.0031	0.0034	0.0033	0.0031
R^2	0.8601	0.8656	0.8426	0.8308	0.7411	0.6991
Dubinin–Radushkevich isotherm						
q_m	7.157	7.211	7.231	7.256	7.278	7.424
β	−0.00038	−0.00036	−0.00031	−0.00023	−0.00015	−0.00017
R^2	0.9227	0.933	0.9244	0.9279	0.9178	0.9207

3.6.3. Temkin isotherm

The Temkin isotherm, assumes that the fall in the heat of sorption is linear and the distribution of binding energies is uniform (up to some maximum binding energy). This model takes into account the presence of indirect adsorbate/adsorbent interactions and suggests that because of these interactions the heat of adsorption of all molecules in the layer would decrease linearly with coverage [36,37]. The Temkin isotherm has generally been applied in the following form:

$$q_e = B \ln K_T + B \ln C_e \tag{10}$$

Table 4
Comparison of adsorption capacities for different adsorbents and dyes

Adsorbent	Adsorbate	q_{max} (mg/g)	References
$MWCNT_S$	Acid Red 18	166.67	[39]
Activated carbon (poplar wood)	Acid Red 18	3.9	[40]
Activated rice husk carbon	Acid yellow 36	86.9	[41]
Penicillium restrictum biomass	Reactive Black 5	98.33	[42]
Raw Kaolinite	Acid Red 18	29	[43]
Montmorillonite	Acid Red 18	19	[43]
Brazilian pine-fruit shell	Reactive Red 194	20.8	[44]
Cumin herb wastes	Reactive Red-120	47.88	[45]
Salvadora persica stems ash	Methylene blue	22.78	[46]
Bone char	Reactive Black 5	160	[47]
Cetyltrimethylammonium bromide modified zeolit	Reactive Black 5	12.93	[48]
High lime fly ash	Reactive Black 5	7.94	[49]
Active carbon F400	Reactive Black 5	176	[50]
Bone char	Reactive Black 5	157	[50]
Peat	Reactive Black 5	7	[50]
Bamboo carbon	Reactive Black 5	447	[50]
Dried activated sludge	Basic Red 29	224.72	[51]
Nickel nanoparticles loaded on activated carbon	Arsenazo (III) dye	168	[52]
Zinc oxide nanoparticles loaded on activated carbon	Bromophenol red	200	[53]
$MWCNT_S$ (at 293 °K)	Reactive Black 5	1,054.05	Present study
$MWCNT_S$ (at 298 °K)	Reactive Black 5	1,082.07	Present study

The constant K_T and B_1 can be calculated using a linear plot of q_e vs. ln C_e. K_T is the equilibrium blinding constant (L/mg) corresponding to maximum binding energy and constant B_1 is related to heat of adsorption. The values are presented in Table 3.

3.6.4. Dubinin–Radushkevich isotherm

The Dubinin–Radushkevich model is often used to estimate the characteristic porosity and the apparent free energy of adsorption. The linear form of Dubinin–Radushkevich isotherm model is:

$$\log q_e = \ln\ q_m - \beta\varepsilon^2 \tag{11}$$

where β is a constant connected with the mean free energy of adsorption per mole of the adsorbate (mol^2/KJ^2), q_m is the theoretical saturation capacity (mg/g), and ε is the Polanyi potential [38].

The isotherms based on the experimental data and the parameters obtained from non-linear regression by four models are presented in Table 3. According to results of this table, the correlation coefficient of the Freundlich model was higher than other models, indicating that the Freundlich model is suitable for describing the adsorption equilibrium of RB5 dye onto MWCNTs. Maximum adsorption capacity of some adsorbents for different dyes was presented in Table 4.

4. Conclusions

In this study, the adsorption of RB5 onto MWCNTs has been investigated. The influence of the important operating parameters, such as pH, contact time, adsorbent dose, initial dye concentration, and temperature on the adsorption of RB5 was investigated. The results show that all the parameters have a strong effect on the adsorption of RB5 onto the adsorbent.

The results demonstrated that adsorption capacity of RB5 on MWCNTs was higher in lower pHs due to significantly high electrostatic attraction that exists between the positively charged surface of the adsorbent and negatively charged anionic dye.

Furthermore, according to results of this study, the MWCNTs were able to remove up to 98% of RB5 dye from solutions whose initial concentration varied between 10–200 mg/L at contact time 60 min. The adsorption of RB5 dye on MWCNTs has been described by the Langmuir, Freundlich, Temkin, and Dubinin–Radushkevich isotherms. It was found that the data fitted well to Freundlich isotherm ($R^2 > 0.99$) better than other isotherms. The removal of the dye from aqueous solutions is induced by adsorption on surface sites of the solid for low RB5 dye concentration, while both adsorption and internal exchange take place for high concentrations.

Acknowledgments

This study was funded by the health research deputy of Zahedan University of Medical Sciences (Project No. 91-2615) and was conducted in the Chemical Laboratory of School of Public Health, Zahedan University of Medical Sciences.

References

[1] G.M.B. Soares, M.T.P. Amorim, R. Hrdina, M. Costa-Ferreira, Studies on the biotransformation of novel disazo dyes by laccase, Process Biochem. 37 (2002) 581–587.
[2] R. Nilsson, R. Nordlinder, U. Wass, Asthma, rhinitis, and dermatitis in workers exposed to reactive dyes, Br. J. Ind. Med. 50 (1993) 65–70.
[3] G. Mezohegyi, A. Kolodkin, U.I. Castro, C. Bengoa, F. Stuber, J. Font, A. Fabregat, A. Fortuny, Effective anaerobic decolorization of azo dye acid orange 7 in continuous upflow packed-bed reactor using biological activated carbon system, Ind. Eng. Chem. Res. 46 (2007) 6788–6792.
[4] T. Satapanajaru, C. Chompuchan, P. Suntornchot, P. Pengthamkeerati, Enhancing decolorization of Reactive Black 5 and Reactive Red 198 during nano zerovalent iron treatment, Desalination 266 (2011) 218–230.
[5] J. Pierce, Colour in textile effluents-the origins of the problem, J. Soc. Dyers Colour 110 (1994) 131–134.
[6] I. Koyuncu, Reactive dye removal in dye/salt mixtures by nanofiltration membranes containing vinylsulphone dyes: Effects of feed concentration and cross flow velocity, Desalination 143 (2002) 243–253.
[7] S. Netpradit, P. Thiravetyan, S. Towprayoon, Application of 'waste' metal hydroxide sludge for adsorption of azo reactive dyes, Water Res. 37 (2003) 763–772.
[8] C. Allègre, P. Moulin, M.F. Maisseu, Treatment and reuse of reactive dyeing effluents, J. Membr. Sci. 269 (2006) 15–34.
[9] S. Yu, M. Liu, M. Ma, M. Qi, Z.L.C. Lü, Impacts of membrane properties on reactive dye removal from dye/salt mixtures by asymmetric cellulose acetate and composite polyamide nanofiltration membranes, J. Membr. Sci. 350 (2010) 83–91.
[10] A. Maleki, A.H. Mahvi, R. Ebrahimi, Y. Zandsalimi, Study of photochemical and sonochemical processes efficiency for degradation of dyes in aqueous solution, Korean J. Chem Eng. 27 (2010) 1805–1810.
[11] S. Sadri Moghaddam, M.R. Alavi Moghaddam, M. Arami, Coagulation/flocculation process for dye removal using sludge from water treatment plant: Optimization through response surface methodology, J. Hazard. Mater. 175 (2010) 651–657.

[12] E. Hosseini Koupaie, M.R. Alavi Moghaddam, S.H. Hashemi, Investigation of decolorization kinetics and biodegradation of azo dye acid red 18 using sequential process of anaerobic sequencing batch reactor/moving bed sequencing batch biofilm reactor, Int. Biodeter. Biodegr. 71 (2012) 43–49.
[13] S. Chatterjee, D.S. Lee, M.W. Lee, S.H. Woo, Enhanced adsorption of congo red from aqueous solutions by chitosan hydrogel beads impregnated with cetyl trimethyl ammonium bromide, Bioresour. Technol. 100 (2009) 2803–2809.
[14] M.R. Samarghandi, M. Zarrabi, M. Noori sepehr, A. Amrane, G. Hossein Safari, S. Bashiri, Application of acidic treated pumice as an adsorbent for the removal of azo dye from aqueous solutions: Kinetic, equilibrium and thermodynamic studies, Iran J. Environ. Health. Sci. Eng. 9 (2012) 101–108.
[15] K.C.L.N. Rao, K.K. Ashutosh, Color removal from a dye stuff industry effluent using activated carbon, Indian. J. Chem. Tech. 1 (1994) 13–19.
[16] J. Hu, Ch Chen, X. Zhu, X. Wang, Removal of chromium from aqueous solution by using oxidized multiwalled carbon nanotubes, J. Hazard. Mater. 162 (2009) 1542–1550.
[17] T. Madrakian, A. Afkhami, M. Ahmadi, H. Bagheri, Removal of some cationic dyes from aqueous solutions using magnetic-modified multi-walled carbon nanotubes, J. Hazard. Mater. 196 (2011) 109–114.
[18] R. Long, R. Yang, Carbon nanotubes as superior sorbent for dioxin removal, J. Am. Chem. Soc. 123 (2001) 2058–2059.
[19] M. Ghaedi, N. Taghavimoghadam, S. Naderi, R. Sahraei, A. Daneshfar, Comparison of removal of bromothymol blue from aqueous solution by multiwalled carbon nanotube and $Zn(OH)_2$ nanoparticles loaded on activated carbon: A thermodynamic study, J. Ind. Eng. Chem. 19(5) (2013) 1493–1500.
[20] M.H. Dehghani, A. Naghizadeh, A. Rashidi, E. Derakhshani, Adsorption of reactive blue 29 dye from aqueous solution by multiwall carbon nanotubes, Des. Wat. Treat. (2013) 1–8.
[21] J.J.M. Órfão, A.I.M. Silva, J.C.V. Pereira, S.A. Barata, I.M. Fonseca, P.C.C. Faria, M.F.R. Pereira, Adsorption of a reactive dye on chemically modified activated carbons—Influence of pH, J. Colloid Interface Sci. 296 (2006) 480–489.
[22] A.S. Özcan, A. Özcan, Adsorption of acid dyes from aqueous solutions onto acid-activated bentonite, J. Colloid Interface Sci. 276 (2004) 39–46.
[23] T. Calvete, E.C. Lima, N.F. Cardoso, S.L.P. Dias, F.A. Pavan, Application of carbon adsorbents prepared from the Brazilian-pine fruit shell for removal of procion red MX 3B from aqueous solution-kinetic, equilibrium, and thermodynamic studies, Chem Eng J. 155 (2010) 627–636.
[24] E. Bazrafshan, F. Kord Mostafapour, H. Faridi, M. Farzadkia, S. Sargazi, A. Sohrabi, Removal of 2,4-Dichlorophenoxyacetic acid (2,4-D) from aqueous environments using single-walled carbon nanotubes, Health Scope 2 (2013) 39–46.
[25] E. Bazrafshan, F. Kord Mostafapour, A.R. Hosseini, A. Rakhsh Khorshid, A.H. Mahvi, Decolorisation of reactive red (120) dye by using single-walled carbon nanotubes in aqueous solutions, J. Chem. 2013 (2013) 1–8.
[26] E. Bazrafshan, F. Kord Mostafapour, A.H. Mahvi, Phenol removal from aqueous solutions using pistachio-nut shell ash as a low cost adsorbent, Fresen. Environ. Bul. 21 (2012) 2962–2968.
[27] S.M. Al-Rashed, A.A. Al-Gaid, Kinetic and thermodynamic studies on the adsorption behavior of Rhodamine B dye on Duolite C-20 resin, J. Saudi. Chem. Soc. 16 (2012) 209–215.
[28] J.F. Osma, V. Saravia, J.L. Toca-Herrera, S. Couto, Sunflower seed shells: A novel and effective low-cost adsorbent for the removal of the diazo dye reactive black 5 from aqueous solutions, J. Hazard. Mater. 147 (2007) 900–905.
[29] Z. Al-Qodah, Adsorption of dyes using shale oil ash, Water Res. 34 (2000) 4295–4303.
[30] M. Khodaie, N. Ghasemi, B. Moradi, M. Rahimi, Removal of methylene blue from wastewater by adsorption onto $ZnCl_2$ activated corn husk carbon, equilibrium studies, J. Chem. 2013 (2013) 1–6.
[31] A.B. Zaki, M.Y. El-Sheikh, J. Evans, S.A. El-Safty, Kinetics and mechanism of the sorption of some aromatic amines onto amberlite IRA-904 anion-exchange resin, J. Colloid. Interf. Sci. 221 (2000) 58–63.
[32] E. Errais, J. Duplay, F. Darragi, I. M'Rabet, A. Aubert, F. Huber, G. Morvan, Efficient anionic dye adsorption on natural untreated clay: Kinetic study and thermodynamic parameters, Desalination 275 (2011) 74–81.
[33] V.K. Gupta, Equilibrium uptake, sorption dynamics, process development, and column operations for the removal of copper and nickel from aqueous solution and wastewater using activated slag, a low-cost adsorbent, Ind. Eng. Chem. Res. 37 (1998) 192–202.
[34] Z. Eren, F.N. Acar, Adsorption of reactive black 5 from an aqueous solution: Equilibrium and kinetic studies, Desalination 194 (2006) 1–10.
[35] W.J. Weber, J.C. Morris, Advances in water pollution research: Removal of bio-logically resistant pollutants from waste waters by adsorption, International Conference on Water Pollution Symposium, vol. 2, Pergamon Press, Oxford, 1962, pp. 231–266.
[36] G. Crini, H.N. Peindy, Adsorption of C.I. basic blue 9 on cyclodextrin-based material containing carboxylic groups, Dyes Pigment 70 (2006) 204–211.
[37] B. Hameed, I. Tan, A. Ahmad, Adsorption isotherm, kinetic modeling and mechanism of 2,4,6-trichlorophenol on coconut husk-based activated carbon, Chem. Eng. J. 144 (2008) 235–244.
[38] M.M. Montazer-Rahmati, P. Rabbani, Kinetics and equilibrium studies on biosorption of cadmium, lead, and nickel ions from aqueous solutions by intact and chemically modified brown algae, J. Hazard. Mater. 185 (2011) 401–407.
[39] M. Shirmardi, A.R. Mesdaghinia, A.H. Mahvi, S. Nasseri, R. Nabizadeh, Kinetics and equilibrium studies on adsorption of acid red 18 (Azo-Dye) using multiwall carbon nanotubes (MWCNTs) from aqueous solution, E-J. Chem. 9 (2012) 2371–2383.
[40] R. Shokoohi, V. Vatanpoor, M. Zarrabi, A. Vatani, Adsorption of acid red 18 (AR18) by activated carbon from poplar wood- a kinetic and equilibrium study, E-J. Chem. 7 (2010) 65–72.

[41] A. Tor, Y. Cengeloglu, Removal of congo red from aqueous solution by adsorption onto acid activated red mud. J. Hazard. Mater. 138(2) (2006) 409–415.
[42] C.F. Iscen, I. Kiran, S. Ilhan, Biosorption of reactive black 5 dye by penicillium restrictum: The kinetic study, J. Hazard. Mater. 143 (2007) 335–340.
[43] H.A. Aydin, O. Yavuz, Removal of acid red 183 from aqueous solution using clay and activated carbon, Indian. J. Chem. Technol. 11 (2004) 89–94.
[44] E.C. Lima, B. Royer, J.C.P. Vaghetti, N.M. Simon, B.M. Da Cunha, F.A. Pavan, E.V. Benvenutti, R.C. Veses, C. Airoldi, Application of Brazilian pine-fruit shell as a biosorbent to removal of reactive red 194 textile dye from aqueous solution, J. Hazard. Mater. 155 (2008) 536–550.
[45] E. Bazrafshan, M. Ahmadabadi, A.H. Mahvi, Reactive Red-120 removal by activated carbon obtained from cumin herb wastes, Fresen. Environ. Bull. 22 (2013) 584–590.
[46] E. Bazrafshan, F. Kord, Mostafapour and M.A. Zazouli, Methylene blue (cationic dye) adsorption into *Salvadora persica* stems ash, Afr. J. Biotechnol. 11 (2012) 16661–16668.
[47] W.M. Alvin, J.P. Barford, G. McKay, A comparative study on the kinetics and mechanisms of removal of reactive black 5 by adsorption onto activated carbons and bone char, Chem. Eng. J. 157 (2010) 434–442.
[48] D. Karadag, M. Turan, E. Akgul, S. Tok, A. Faki, Adsorption equilibrium and kinetics of Reactive Black 5 and reactive red 239 in aqueous solution onto surfactant-modified zeolite, J. Chem. Eng. 52 (2007) 1615–1620.
[49] Z. Eren, F.N. Acar, Equilibrium and kinetic mechanism for Reactive Black 5 sorption onto high lime soma fly ash, J. Hazard Mater. 143 (2007) 226–232.
[50] A.W.M. Ip, J.P. Barford, G. McKay, Reactive Black dye adsorption/desorption onto different adsorbents: Effect of salt, surface chemistry, pore size and surface area, J. Colloid Interface Sci. 337 (2009) 32–38.
[51] H.C. Chu, L.H. Lin, H.J. Liu, K.M. Chen, Utilization of dried activated sludge for the removal of basic dye from aqueous solution, Desal. Wat. Treat. 51 (2013) 7074–7080.
[52] F. Taghizadeh, M. Ghaedi, K. Kamali, E. Sharifpour, R. Sahraie, M.K. Purkait, Comparison of nickel and/or zinc selenide nanoparticle loaded on activated carbon as efficient adsorbents for kinetic and equilibrium study of removal of Arsenazo (III) dye, Powder. Technol. 245 (2013) 217–226.
[53] M. Ghaedi, M. Ghayedi, S.N. Kokhdan, R. Sahraei, A. Daneshfar, Palladium, silver, and zinc oxide nanoparticles loaded on activated carbon as adsorbent for removal of bromophenol red from aqueous solution, J. Ind. Eng. Chem. 19(4) (2013) 1209–1217.